# CHAPTER II

BACKGROUND AND LITERATURE SURVEY

2.1 Matrix Acidization

Matrix acidization is a well stimulation technique commonly applied to sandstone reservoirs. The simple objective of matrix acidization is to improve the oil productivity by injecting acid mixtures into reservoirs to remove formation damage and create a high-permeability network around the wellbore (Economides *et al.*, 1988; Crowe, 1992).
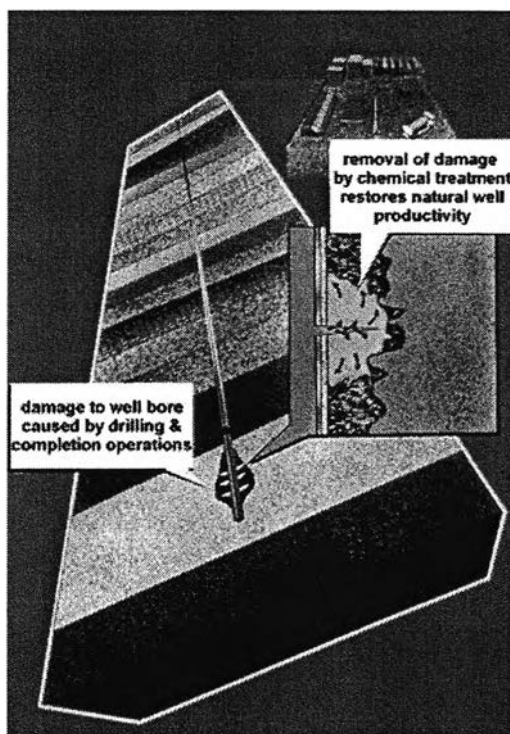
Figure 2.1 Matrix acidization
(http://www.gidatec.co.uk/Wellstimulation.htm).

For sandstone formations, the matrix acidization commonly consists of 3 stages: preflush, main flush, and postflush or overflush. During the preflush stage, a preflush fluid, a solution containing 5-15% hydrochloric or acetic acid, is pumped

into the formation to remove calcium carbonate, and displace formation fluid away from the wellbore to allow the main-stage fluid (mud acid – an acid containing 12% HCl and 0.5-3% HF) to react with existing minerals. An overflush fluid is then injected into the well to displace non-reacted mud acid and reaction products away from the bore hole (McLeod and Norman, 2000).

A set of reactions can take place when spent acid contracts silicate and other minerals, leading to precipitation of siliceous product. Therefore, working on acidizing in sandstone reservoirs requires special attention (Underdown *et al.*, 1990; Coulter and Jennings, 1999).

2.2 Analcime Dissolution

Analcime (or analcite) is a hydrous sodium aluminosilicate mineral. The unit-cell formula can be written as $16(NaAlSi_2O_6 \cdot H_2O)$, and the Si to Al ratio of analcime is ideally two. Analcime is a naturally occurring zeolite, which can be found in geological formations worldwide including Scotland, Iceland, United States, Canada, Australia, and India (King, 2001).

Analcime dissolution phenomena in acid solutions have been recently investigated. The dissolution of analcime in hydrochloric acid is suggested to obey the following reaction:

$$Na_2O \cdot Al_2O_3 \cdot 4SiO_2 \cdot 2H_2O + 8HCl + 2H_2O \rightarrow 2AlCl_3 + 2NaCl + 4Si(OH)_4 \qquad (2.1)$$
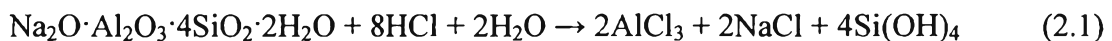
where the products are aluminum chloride, sodium chloride, and monosilicic acid.

Preliminary studies showed that the initial rates of analcime dissolution in HCl, HBr, HI, and HNO_3 follow the Michaelis-Menten equation analogous to Langmuir-Hinshelwood kinetics under low pH and temperature (Hartman, 2006; Hassan, 2007). The initial rate law is simply written as:

$$- r_{i,0} = \frac{V_{max}[H^+]}{K_m + [H^+]} \qquad (2.2)$$

where $\quad V_{max} = k_3[S_T] \quad$ = maximum dissolution rate, $\qquad (2.3)$

$$K_m = \frac{k_2 + k_3}{k_1} \quad = \text{Michaelis-Menten constant}, \qquad (2.4)$$

$[H^+]$ = hydrogen-ion concentration,

and $\quad [S_T]$ = concentration of active sites.

The proposed dissolution mechanism involves a reversible hydrogen-ion sorption and subsequent surface reaction as shown in Figure 2.2. The dissolution occurs when hydrogen ions attack oxygen-aluminum bonds on the analcime framework, resulting in the release of silicon compounds. Once dissolved, silicon polymerizes and eventually forms a gel/precipitate (Gorrepati and Fogler, 2008).
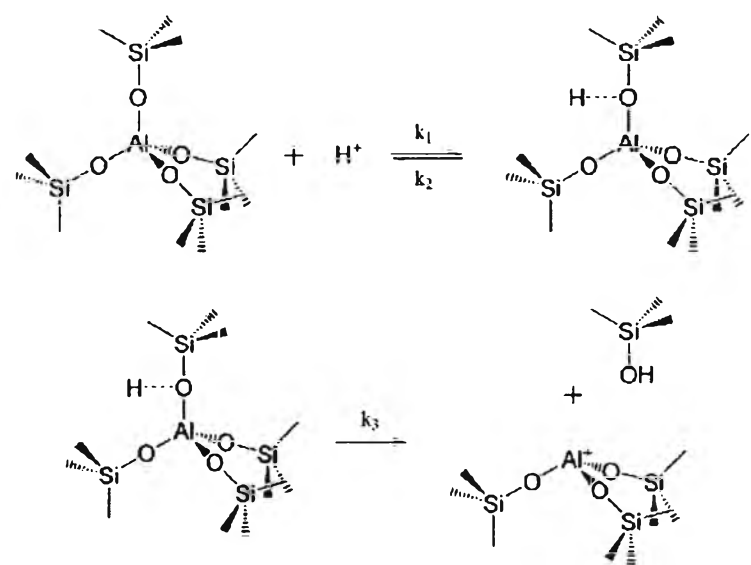
Figure 2.2 Reaction scheme representing the dissolution of analcime framework in HCl; Hydrogen-ion sorption (top) and Surface reaction (bottom) (Hartman and Fogler, 2007).

2.3 Silica polymerization/Precipitation

Silica precipitate is primarily created through the condensation polymerization of a supersaturated monosilicic acid solution, forming silica particle nuclei, which is followed by growth of silica particles by chemical deposition of silicic acid on their surfaces. This may then be followed by the formation of large colloidal particles by coagulation or flocculation in order to form a gel/precipitate. The gel formation/precipitation is depended on pH, temperature, degree of supersaturation, and salinity due to the presence of other substances (Goto, 1956; Iler, 1979; Weres et al., 1981).
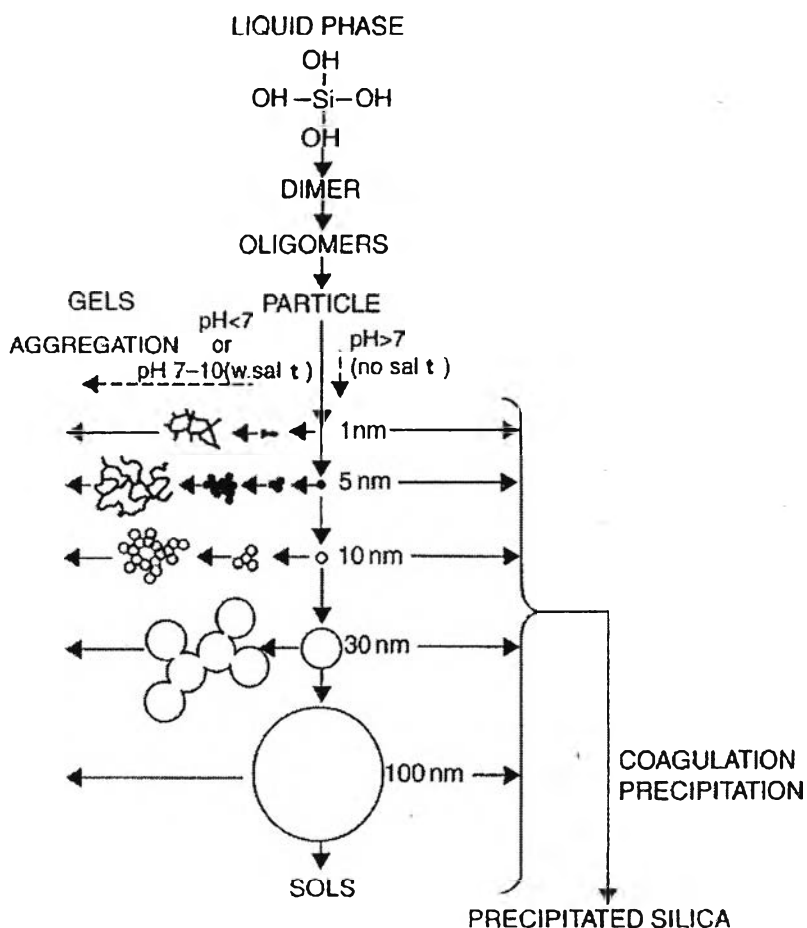
**Figure 2.3** Polymerization behavior of silica (Iler, 1979).

Silica polymerization begins with the condensation of monosilicic acid to form cyclic oligomers, which then polymerize into chains and three-dimensional networks that can function as nuclei with radii of the order of a few angstrom. These nuclei may remain dispersed for long periods of time until condensation reactions cause coalescence and precipitation from solution (Makrides *et al.*, 1980; Icopini *et al.*, 2005).

Most experimental studies of silica polymerization in relatively dilute solutions of geological interest have involved measuring concentrations of silicic acid monomer in solution (Perry and Keeling-Tucker, 2000). Many have studied the polymerization kinetics in supersaturated solutions near ambient temperature. Nonetheless, the available literature presents an inconsistency in the reaction orders of monosilicic acid polymerization. Among a variety of experimental conditions, a maximum rate between $6 < pH < 9$ and reaction order of 1 to 8 have been reported, indicating that kinetics of monosilicic acid condensation and precipitation are still ambiguous (Alexander, 1954; Wirth and Geiske, 1979; Perry and Keeling-Tucker, 2000; Icopini *et al.*, 2005).

In the petroleum industry, silica precipitated as a result of acid treatments has been referred to as "hydrated silica" or a "colloidal silica gel" (Underdown *et al.*, 1990; Gdanski, 2000). These terms all describe hydrated silica gels or amorphous precipitates that result from acidization treatments. Gorrepati and Fogler (2008) investigated silica precipitation of analcime during matrix acidization. Pure monosilicic acid was used as a Si source of precipitation experiments because it was shown that monosilicic acid can mimic the silica precipitation after analcime dissolution. It was found that the polymerization of monosilicic acid took place rapidly via a second order rate law. After a short period of time, primary silica particles of ~5nm were formed and those particles started to grow exponentially by aggregation/flocculation. Furthermore, increasing HCl concentrations can promote the particle growth rate as well as the silicic acid monomer disappearance rate.

2.4 Ionic Effects on Silica Precipitation Phenomena

Ionic effects on silica systems in *mildly acidic to alkaline* systems have been extensively studied in terms of ionic strength and the presence of salt. Recent studies have revealed that the rate of silica polymerization increases with higher ion strength. In addition, it has been shown that the rate of precipitation (polymerization) of silicic acid increases with increasing salt concentration (Makrides *et al.*, 1980; Fleming 1986; Icopini *et al.*, 2005). Marshall and Warakomski (1990) reported that the rate of polymerization in *circum-neutral* solutions with cations follow the order of:

$$Mg^{2+} > Ca^{2+} > Sr^{2+} > Li^+ > Na^+ > K^+,$$
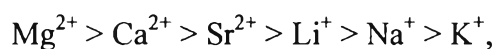
and for anions was found as:

$$I^- > Br^- > Cl^-.$$
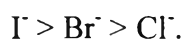
The rankings of those ions are only valid for a given set of conditions and depended on the change in experimental conditions. However, the basic mechanism by which salts accelerate silica precipitation is still unknown.

2.5 Aggregation Modeling: Smoluchowski Aggregation Approach

The aggregation of particles was first described by von Smoluchowski (1917). A fundamental assumption of the Smoluchowski approach is that aggregation is a second-order rate process where the rate of collision is proportional to the product of the concentration of the two colliding species, simply referred as the 'i-th' and 'j-th' aggregates. The Smoluchowski equation for the k-th aggregate having k number of primary units, where k = i + j, is given as (Elimelech *et al.*, 1995)

$$\frac{dn_k}{dt} = \frac{1}{2} \sum_{\substack{i+j \to k \\ i=1}}^{i=k-1} K_{ij} n_i n_j - n_k \sum_{k=1}^{\infty} K_{ik} n_i$$

(2.5)

where k   = the number of aggregate unit (k=1,2,3,..N),

         n_i = molar concentration of i-th aggregates ($\frac{mol}{dm^3}$),

and K_{ij} = collision kernel ($\frac{dm^3}{mol \cdot s}$).

The first term represents the rate of formation of k-th aggregates through binary collision of smaller aggregates, and the second term accounts for the loss of k-th aggregates by colliding with any other aggregates. The collision kernel is a parameter related to the rate constant. K_{ij} denotes the collision kernel describing the rate at which i-th aggregate coagulates with j-th aggregate.

To solve the population balance equation (2.5) for each species, the Smoluchowski equation is computationally expensive and becomes impractical when particles vary over a wide range of size (see *Table 2.1*). A geometric scaling approach has been applied to the population balance equation in order to reduce the computational intensity of the Smoluchowski equation by reducing the number of governing ordinary differential equations based on a geometric scaling of R, where R is a geometric spacing between two subsequent aggregates (Hounslow *et al.*, 1988; Maqbool *et al.*, 2007). The geometric population equation is used only for aggregates with a geometric number of primary units of R^{j-1}, where j is the number of aggregate unit. For example for the case of R=2, the fifth aggregate of the discretized system (j=5) has 2^4 (=16) number of primary units. The number of primary units in an aggregate, n_a is scaled as (Rastegari *et al.*, 2004),

$$n_a \approx \left(\frac{d_a}{d_p} \right)^{D_f}$$

(2.6)

where D_f = fractal dimension of the aggregate,

d_a = aggregate diameter (m),

and d_p = primary unit diameter (m).

Using Equation (2.6), n_a for different situations of D_f, d_a, and d_p are approximated and shown in Table 2.1. In the Smoluchowski concept, n_a number of ordinary differential equations are required to be solve simultaneously. For the sake of comparison between Smoluchowski approach and geometric scaling approach, the numbers of ODE to be solved for geometric scaling and for Smoluchowski idea are compared in Table 2.1.

Table 2.1 Comparison of number of ODEs under different hypothetical scenario (Maqbool *et al.*, 2007).

| Case | Diameter, m | | D_f | n_a | Number of ODEs | |
	Primary unit diameter, d_p	Largest aggregate diameter, d_a			Smoluchowski approach	Geometric scaling approach (R=2)
1	1×10^{-9}	1×10^{-5}	3	1.0×10^{12}	1.0×10^{12}	41
2	1×10^{-9}	1×10^{-6}	2	1.0×10^{8}	1.0×10^{8}	28
3	1×10^{-6}	1×10^{-4}	1.6	1.6×10^{3}	1.6×10^{3}	12

In addition, the generation and depletion terms in equation (2.5) have been modified to become

$$\frac{dn_i}{dt} = \frac{K_{i-1,i-1}}{R} n_{i-1}^2 + n_{i-1}\sum_{j=1}^{i-2}\frac{R^{j-1}}{R^{i-1}-R^{i-2}}K_{i-i,j}n_j - n_i\sum_{j=1}^{i-1}\frac{R^{j-1}}{R^i-R^{i-1}}K_{i,j}n_j - n_i\sum_{j=1}^{N-1}K_{i,j}n_j$$

(2.7)

| Term I | Term II | Term III | Term IV |

Term I: R number of (i-1)-th aggregates to form one i-th aggregate.

Term II: An i-th aggregate to be created by the collision between one (i-1)-th aggregate and $\dfrac{R^{i-1}-R^{i-2}}{R^{j-1}}$ number of j-th aggregates (j<i-1).

Term III: An i-th aggregate reacting with $\dfrac{R^i-R^{i-1}}{R^{j-1}}$ j-th aggregates to form the (i+1)-th aggregates.

Term IV: The formation of one (j+1)-th aggregate by one j-th aggregate (j≥i) and $\dfrac{R^j-R^{j-1}}{R^{i-1}}$ i-th aggregates.

Aggregation phenomena can be categorized into 2 different types: Diffusion-Limited Aggregation (DLA) and Reaction-Limited Aggregation (RLA). DLA occurs when there is a purely attractive force between the colloidal particles. The particle undergoes continuous random movement and sticks irreversibly to the aggregate. In another words, every collision between aggregates or primary particles is successful. The aggregation rate is limited solely by the time required for the aggregates to encounter each other by diffusion (Lin *et al.*, 1989; Elimelech *et al.*, 1995). The growth of the particle obeys power law kinetics. This type of aggregation can be observed in asphaltene systems (Maqbool *et al.*, 2007). RLA happens when there is a substantial amount of repulsive forces between two colliding particles. That is, one particle requires a longer time to overcome this repulsive barrier to collide with another particle. The particle growth is exponential with aggregate size increasing. RLA can be seen in silica, gold, and polystyrene systems (Schaefer *et al.*, 1984; Ball *et al.*, 1987).
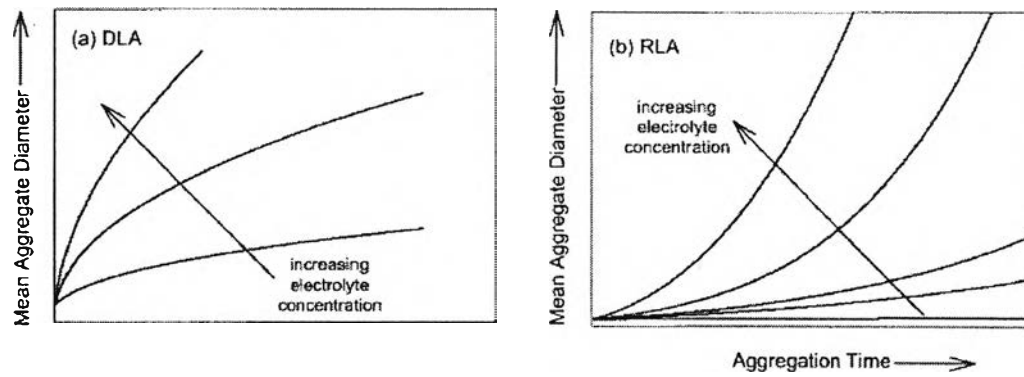
Figure 2.4 Representative particle growth profiles in accord with (a) DLA and (b) RLA (Rungkana *et al.*, 2004).